

Improved energy resolution for VHE gamma-ray astronomy with systems of Cherenkov telescopes

W. Hofmann*, H. Lampeitl, A. Konopelko, H. Krawczynski

*Max-Planck-Institut für Kernphysik, P.O. Box 103980, D-69029 Heidelberg,
Germany*

**Corresponding author (Werner.Hofmann@mpi-hd.mpg.de
Fax +49 6221 516 603, Phone +49 6221 516 330)*

Abstract

We present analysis techniques to improve the energy resolution of stereoscopic systems of imaging atmospheric Cherenkov telescopes, using the HEGRA telescope system as an example. The techniques include (i) the determination of the height of the shower maximum, which is then taken into account in the energy determination, and (ii) the determination of the location of the shower core with the additional constraint that the direction of the gamma rays is known a priori. This constraint can be applied for gamma-ray point sources, and results in a significant improvement in the localization of the shower core, which translates into better energy resolution. Combining both techniques, the HEGRA telescopes reach an energy resolution between 9% and 12%, over the entire energy range from 1 TeV to almost 100 TeV. Options for further improvements of the energy resolution are discussed.

Imaging atmospheric Cherenkov telescopes (IACTs) represent the prime instruments for gamma-ray astronomy in the TeV energy range [1]. With a number of sources established as TeV gamma-ray emitters in IACT observations, emphasis is starting to shift from the pure detection of sources to the precise determination of gamma-ray spectra. The energy of gamma rays is determined from the intensity of IACT images, taking into account the radial distribution of Cherenkov light within the light pool. In case of stereoscopic systems of multiple IACTs, which observe an air shower from different viewing angles, the location of the shower axis and hence the distance of a given telescope from this axis can be obtained by a simple geometrical reconstruction. For single IACTs, the impact distance can be estimated based on the location and shape of the Cherenkov image within the camera, albeit with larger uncertainty. Energy resolutions quoted around 1 TeV for single telescopes vary between 29%-36% [2,3], \approx 30-35% [4] and 20-28% [5]. The HEGRA systems of IACTs provides a resolution of about 20% [6].

Sources such as the Crab Nebula or the AGN Mkn 421 show spectra which are consistent

with pure power laws, $dN/dE \sim E^{-\alpha}$, with spectral indices α ranging between 2.5 and about 4. In the determination of power-law energy spectra, energy resolution is not a very critical parameter. Convolution of a power-law spectrum with a resolution function of constant width $\Delta E/E$ will result in a spectrum with the identical spectral index. A correction is required in the determination of the flux at or above a certain energy, but this correction is modest even for instruments with a poor resolution $\Delta E/E \approx 40\%$.

The situation changes once sources exhibit a cutoff in the energy spectrum, such as observed for Mkn 501 [3,7,8,4,6]. For the interpretation of the cutoff phenomenon, e.g. in terms of absorption of gamma rays in interactions with the infrared/optical background, it is important to precisely map the shape of cutoff. Smearing of the spectrum with an energy resolution in the 20% range may distort its shape significantly. In principle, the original spectrum can be recovered by unfolding techniques (see, e.g., [4] and refs. given there). However, all such techniques result in rapidly increasing statistical errors, once the bin size of the unfolded spectrum approaches the energy resolution of the instrument – after all, the loss of information cannot be recovered and leads to this penalty.

It is therefore of significant importance to improve the energy resolution of IACTs. In this article, we will demonstrate that with new analysis techniques, a significant improvement of the energy resolution of stereoscopic systems of IACTs can be achieved, in particular if the source of gamma rays can be considered a point source with known position. The results are based on Monte-Carlo simulations of the HEGRA IACT system, but they should apply in similar form to the various new systems of IACTs which are currently planned or in construction.

1 Factors governing the energy resolution of Cherenkov telescopes

The energy resolution of Cherenkov telescopes is governed by a number of factors, among them

Statistical fluctuations in the image. Since the number of photoelectrons in a typical image is $O(100)$, statistical fluctuations in the number of photoelectrons limit the resolution to $O(10\%)$. Additional fluctuations arise from the amplification process in the photomultiplier and from night-sky background under the image. In case of the HEGRA telescopes, the amplification noise increases the fluctuations by a about a factor 1.2 compared to the Poisson fluctuations alone, and the night-sky noise in a typical image corresponds to about 4-5 p.e. rms.

Image truncation. In order to reduce the influence of the night-sky background, the image intensity is usually summed only over ‘image pixels’ above a minimum intensity, cutting away the tail of the image. The sum over image pixel amplitudes provides the so-called *size* parameter used to derive the shower energy. Such a ‘tail cut’ introduces both additional noise as well as systematic nonlinearities; for low-intensity images a larger fraction of the image is cut than for intense images. An additional truncation occurs for images which extend beyond the edge of the camera. At the 10%-level, edge effects start to matter at distances as large as 0.8° between the image centroid and the edge of the camera.

Threshold effects. In the region near the trigger threshold – in case of the HEGRA telescopes this corresponds to images with around 40 p.e. – the image intensity detected in the camera will be strongly biased, since showers with upward fluctuations in the image *size* will have a larger probability of triggering. In the sub-threshold energy region, the mean intensity of triggered images will approach a constant, independent of the shower energy, making an energy determination impossible.

Errors in the localization of the shower core. To convert the measured image intensity into a shower energy, the distance between the telescope and the shower axis needs to be known. For the HEGRA system, the core is located with a precision of 10 m to 20 m, depending on the core distance. In particular for telescopes beyond the Cherenkov radius of about 120 m, where the light intensity varies rapidly with core distance, the resulting uncertainty in the energy estimate may exceed 30%.

Fluctuations in the shower development. Variations in the shower development provide a significant contribution to the energy resolution; particularly relevant are fluctuations in the height of the shower maximum, related primarily to the fluctuation in the depth of the first interaction. Showers with their maximum deeper in the atmosphere have a higher intensity of light within their light pool, both because of the smaller distance between the telescope and the light source, and because of the lower Cherenkov threshold at reduced height.

Systematic errors. All techniques for energy determination rely heavily on Monte-Carlo simulations to provide the relation between image parameters and shower energy, and to describe the performance of the telescope hardware. Imperfections in the simulations of the air shower, or of the telescopes, or alignment errors and calibration errors not included in the simulations may have a detrimental effect on the energy resolution. Great care must be taken to ensure that the simulations properly reproduce all relevant aspects of the data.

Monte Carlo statistics. Algorithms for energy reconstruction frequently use multi-dimensional lookup tables to convert values of image parameters into energy estimates. Given the time-consuming generation of Monte-Carlo events in particular at the higher energies, the number of Monte-Carlo events is frequently similar to, or even inferior to the number of showers detected in the experiment. Statistical errors in the table values may be significant. They can be alleviated by an efficient choice of variables, and by appropriate smoothing of the tables or fitting with a smooth analytical function.

In this paper, we will concentrate on improvements of the energy resolution due to two factors, namely the experimental determination of the height of the shower maximum on an event-by-event basis, and an improved algorithm for the determination of the shower core, applicable for gamma-ray point sources.

Additional improvements should be possible with an improved image analysis, e.g. by fitting image templates to the observed images to properly account for and compensate the truncation effects mentioned above. The detailed discussion of such effects goes beyond the scope of the current work.

2 The HEGRA IACT system, its modeling, and data analysis

The analysis techniques presented on the following have been developed using Monte Carlo simulations of the HEGRA IACT system. The HEGRA IACT system is located at 2.2 km asl. on the Canary Island La Palma, at the Observatorio del Roque de los Muchachos. The stereoscopic IACT system consists of five telescopes, four arranged in the corners of a square with 100 m side length and one in the center. Since the final telescope - one of the corner telescopes - was added rather late to the system, most of the data taken so far use only four telescopes; the Monte Carlo simulations were therefore also restricted to four telescopes. Each of the HEGRA telescopes has 8.5 m² mirror area, 5 m focal length, and is equipped with a 271 pixel camera with a 4.3° field of view. Shower signals in at least two telescopes are required to trigger the system. Details about the telescopes, their trigger system and their performance can be found in [9–11,6].

The Monte Carlo simulations of the HEGRA telescopes are described in [12]. The simulations provide a detailed account both of the evolution of air showers and of the telescope hardware, including a detailed modeling of the optical path and the detection of photons, and of the electronics signal processing by a 120 MHz Flash-ADC system. Simulated events are passed through the same full reconstruction chain as is used for real data.

In order to test the algorithms for the reconstruction of the height of the shower maximum, the Monte Carlo was modified to output the number of Cherenkov photons generated as a function of atmospheric depth. To define the maximum emission, a smooth function was fit to the depth profile. When the term ‘height of the shower maximum’ is used in the following, it refers to the height of maximum emission of Cherenkov photons rather than to the height with maximum number of shower particles. Because of the variation of atmospheric density with height, the maximum Cherenkov emission occurs below the maximum in terms of particle number. Values given for the shower height always refer to the height above the telescopes.

Unless otherwise mentioned, studies were carried out for vertical showers.

The data analysis chain and the cuts are similar, but not identical to those used in [6]). The location of the shower axis, required as input for any energy determination, was determined by geometrical reconstruction; in case events are overconstrained (observation by three or more telescopes), images were combined taking the errors on the image parameters into account (Algorithm 2 of [14]), and cuts were applied on the resulting χ^2 to reject the small fraction of poorly reconstructed events. Only events with cores reconstructed within 200 m from the central telescope were accepted. For the energy reconstruction, only telescopes were used which fulfill the following criteria: (i) at least 40 photoelectrons in the image, (ii) the distance between telescope and shower core does not exceed 200 m, and (iii) in order to exclude images truncated by the edge of the cameras, the image centroid had to be within 1.5° from the camera center. At least two telescopes had to be available for the energy determination.

3 Influence of fluctuations in the shower height on the energy determination

The influence of the height of the shower maximum on the Cherenkov light yield is illustrated in Fig. 1, which displays the light yield observed in a Cherenkov telescope at different distances from the shower axis as a function of the height of the shower maximum above the telescopes. At TeV energies, the average height of the shower maximum is about 6 km, with an rms variation of 800 m, roughly corresponding to one radiation length. The dominant contribution to this variation comes from the fluctuation in the depth of the first interaction. The influence of the height of the maximum on the light yield is dramatic at small distances from the shower axis, decreases smoothly out to the Cherenkov radius of 120 m, and is modest at larger distances.

The variation in the height of the shower maximum is by far the dominant contribution to the fluctuations of the photon density on the ground. This is illustrated in Fig. 2, where the distribution of photons is shown for two simulated showers, normalized to the mean photon density obtained by averaging over many events. The first event, with a low shower maximum, shows a strong enhancement of photon density for radii below 80 m; in the second event, with a high shower maximum, the photon density is reduced in this area. In both events, the distribution of photons is rather smooth¹ and symmetric about the shower axis, indicating that the height of the shower maximum influences the light distribution in a very global fashion, and that other, more local fluctuations are less important. This observation implies that one should be able to rather efficiently correct for the fluctuation of the shower maximum, provided that this quantity can be measured on an event-by-event basis.

In fact, the development of the analysis technique described in this paper was triggered by the experimental observation of such global fluctuations of the light yield [13]: for air showers observed simultaneously by all four of the HEGRA telescopes, the energies determined independently by two subsystems of two telescopes each agreed significantly better than expected under the assumption of uncorrelated measurements, indicative of a common factor influencing both measurements.

4 Reconstruction of shower height

To correct for the dependence of light yield on the height of the shower maximum, this height has to be determined from the information contained in the multiple images. To a first approximation, one may assume that the image of the shower maximum coincides with the centroid of the Cherenkov image. Denoting by h_{max} the height of the shower maximum, by r the distance from the telescope to the shower axis, and by d the distance in the image plane between the

¹ Statistical fluctuations in the light yield are negligible on this scale, given that each bin represents an area of 10 m x 10 m and contains $O(10^4)$ photons per event.

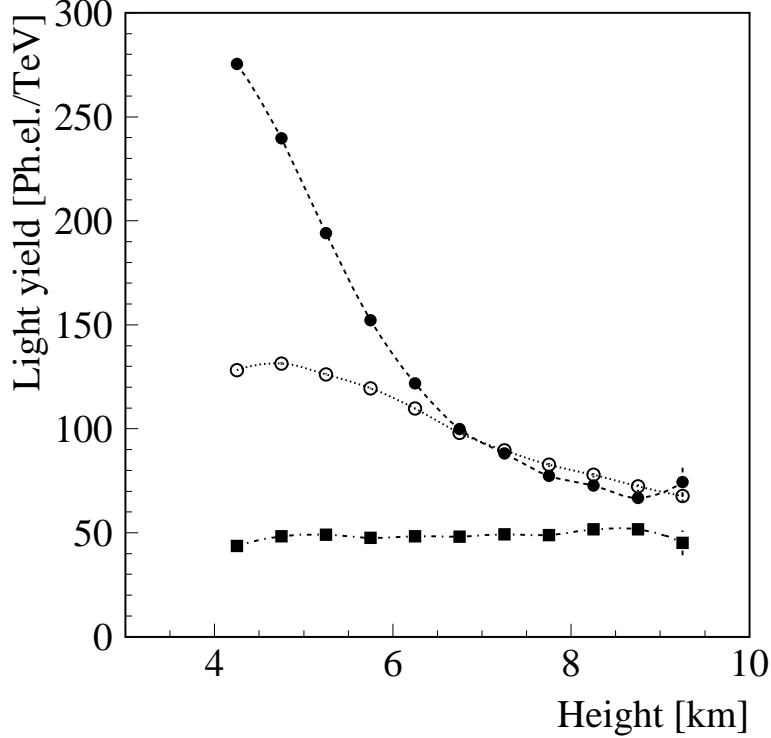


Fig. 1. Light yield detected by the Cherenkov camera as a function of the (measured) height of the shower maximum, at distances of 40-50 m from the center of the light pool (full circles), 90-100 m (open circles), and 140-150 m (full squares), based on Monte Carlo simulations. The light yield is given in units of photoelectrons/TeV.

centroid of the image and the image of the source (in units of degrees²), one finds

$$\frac{1}{h_{max}} = \frac{\pi}{180^\circ} \frac{d}{r} .$$

With a single image, r and h_{max} cannot be determined separately. With a stereoscopic IACT system, r is obtained from the geometrical reconstruction of the shower axis and then an estimate for h_{max} can be obtained for each image, and be suitably averaged over telescopes. Note that measurement errors tend to be Gaussian in d , hence one should average the estimates of $1/h_{max}$.

Monte Carlo simulations show, however, that this model is oversimplified; while light detected at large radii, beyond the Cherenkov radius, is predominantly generated around the shower maximum, light detected at smaller distances from the shower core is generated deeper in the atmosphere. In general, the relation between d and h_{max} can be parameterized as

$$\frac{1}{h_{max}} = c_1(r) + c_2(r) \frac{\pi}{180^\circ} \frac{d}{r} ,$$

² Coordinates in the camera plane are expressed in units of degrees and represent the slope of photon trajectories relative to the telescope axis; they should not be confused with the orientation angle of images within the camera.

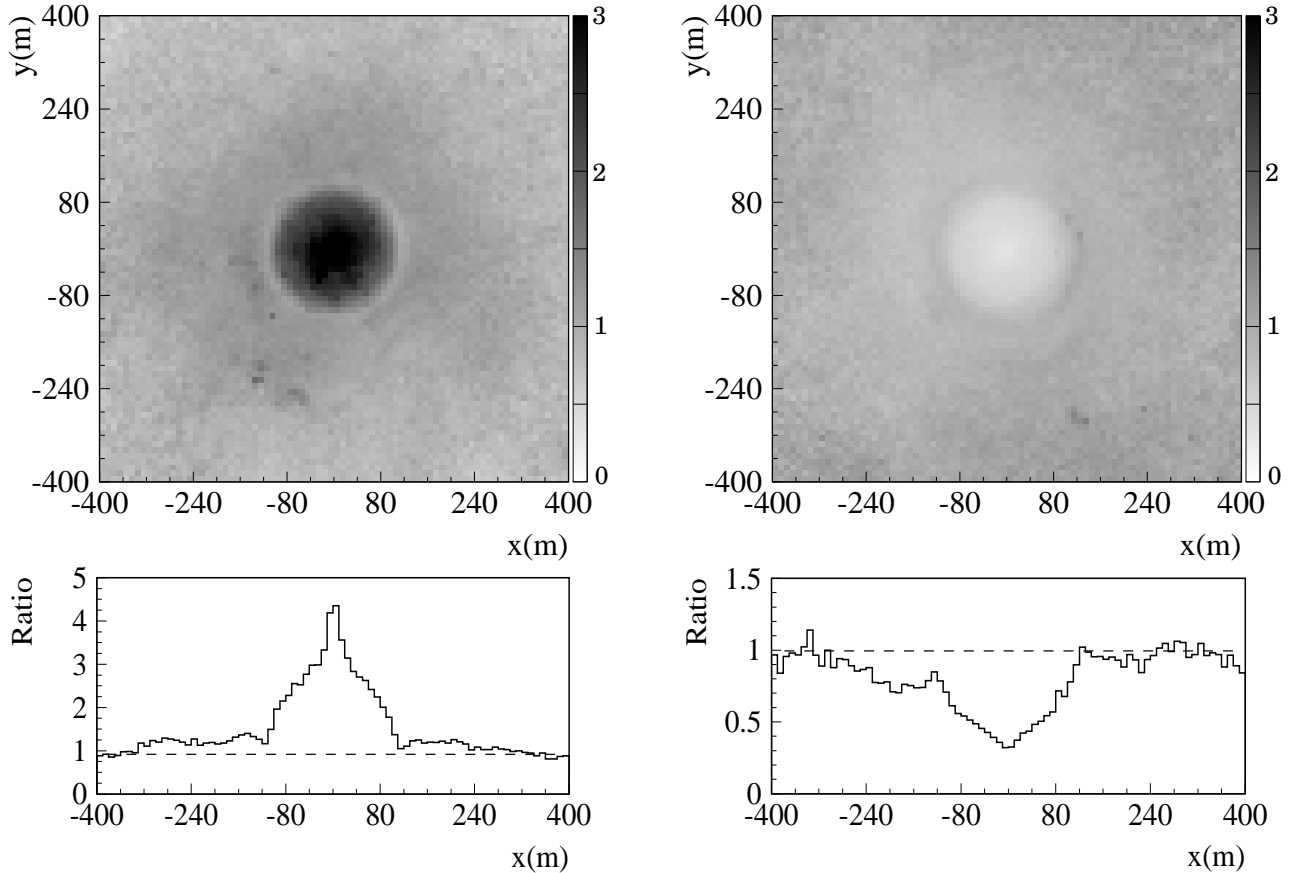


Fig. 2. Photon density on the ground for two selected 1 TeV gamma ray showers, normalized to the average photon density. The shower axis intersects the ground level at $x = y = 0$. The lower panels show a cross section along the x axis, at $y = 0$.

with a small offset c_1 of at most 0.1/km and c_2 rising at small r , leveling off at about unity beyond the Cherenkov radius. Tests showed that in the reconstruction of the shower height, c_1 could be neglected. For c_2 , a simple parameterization was used, see Fig. 3. The values determined for $1/h_{max}$ from the individual telescopes were averaged, assigning to d an error

$$\Delta d = \max\left(\frac{2.5}{\sqrt{I}}, 0.15\right) [degr.] .$$

Here, I denotes the image *size* defined as the sum of the amplitudes of image pixels. Fig. 4 illustrates the distribution of measured height of the shower maximum vs. the true height, for events reconstructed based on two or more telescopes. With the standard reconstruction of the shower geometry, an rms resolution in the height of the maximum of about 600 m is achieved, corresponding to about 0.7 radiation lengths. With the improved determination of the core location (see below), a resolution of about 530 m is obtained.

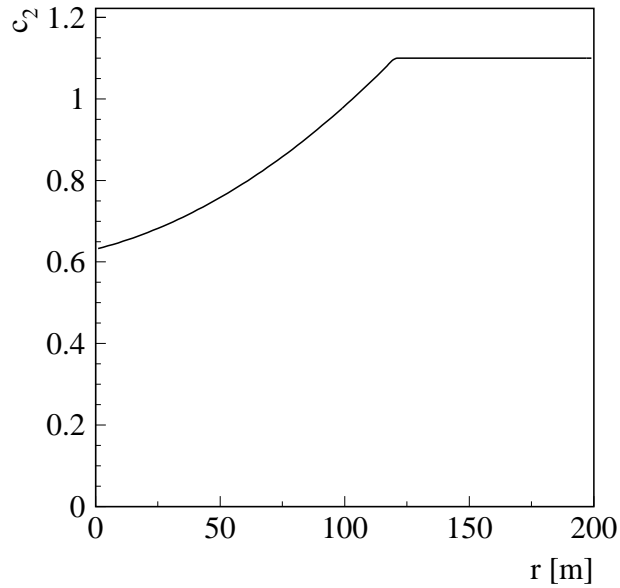


Fig. 3. Coefficient $c_2(r)$ relating the height of the shower maximum to the distance d between the image of the source and the image centroid.

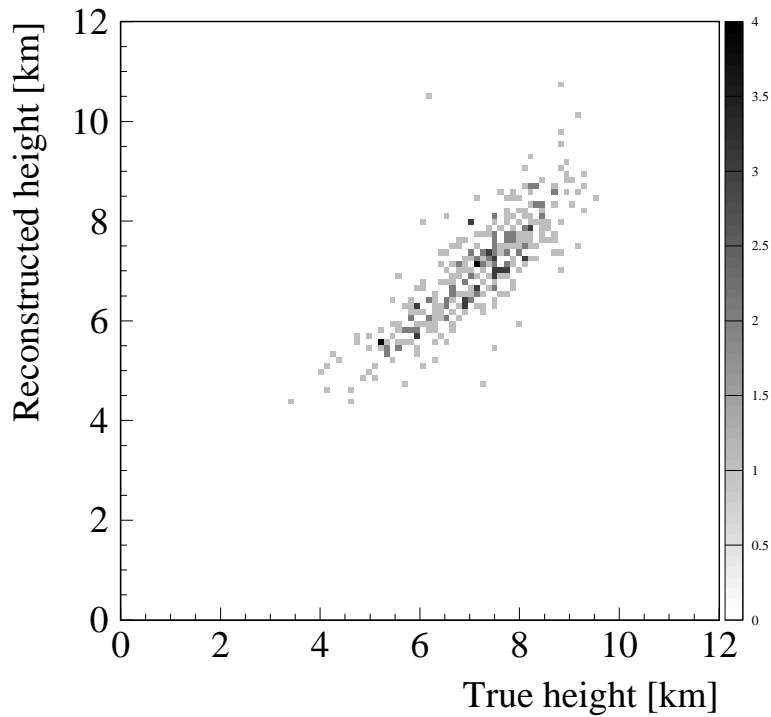


Fig. 4. Distribution of the measured height of the shower maximum vs. the true height, for simulated gamma-ray showers at TeV energies.

5 Improved determination of core location

In the geometrical reconstruction of the geometry of air showers on the basis of multiple stereo views, the dominating source of measurement errors is the uncertainty in the determination of

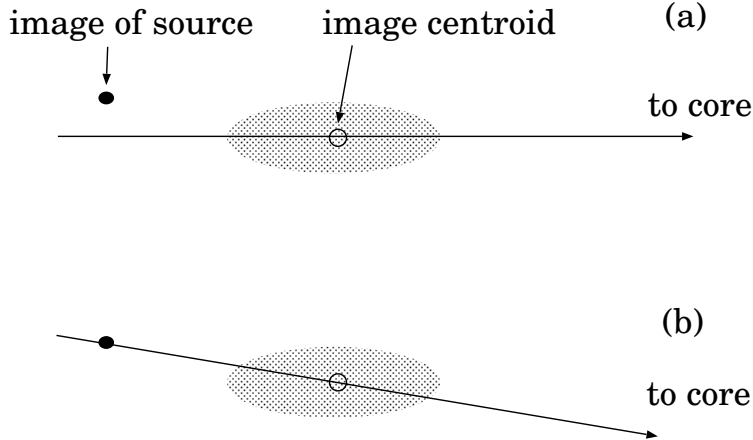


Fig. 5. (a) Normal reconstruction of the core location based on the assumption that the image axis points to the location where the shower axis intersects the plane of the telescope dish. With stereoscopic observation of a shower by two telescopes, the impact point can be determined by intersecting the image axes, starting from the telescope locations. (b) Reconstruction of the core location assuming that the gamma-ray comes from the known point source, and using the vector from the source to the centroid of the image to define the direction to the core. In contrast to the image orientation, the image centroid is usually quite well determined, and therefore the technique (b) usually provides a much better estimate of the direction to the core.

the orientation of the images, with a typical error of about 4° for gamma-ray images containing 100 photoelectrons, detected in the HEGRA cameras. The image centroid is located with a precision of 0.02° , in the direction transverse to the image axis. The high precision in the location of the centroid opens the way to an improved determination of the shower core, for gamma-rays emitted from a point source. For a known source location, the image orientation can be recalculated using the measured position of the image centroid, see Fig. 5 (see also [17]). With a typical distance of 1° between the image of the source and the centroid of the Cherenkov image, the image orientation can be derived with an uncertainty of about 1° , four times better than from the image alone. These improved values provide then the input for the determination of the core location. The resolution in the core coordinates is illustrated in Fig. 6; indeed, one finds that the resolution, which normally varies between 6 m and 10 m in each coordinate, is improved to values between 1.5 m and 3 m.

6 Energy determination

The standard procedure to reconstruct gamma-ray energies using the HEGRA IACT system uses look-up tables to relate the shower energy to the image *size* value I measured at a certain distance from the shower axis. The look-up tables store the mean *size* $I(E, r)$ for 18 bins in core distance, and 16 bins in energy, derived from Monte Carlo simulations. The relation between *size* and energy is nonlinear, because of the effects of tail cuts and since the mean depth of the shower maximum varies with energy. For a given event, for each telescope an energy value is derived by suitable interpolation of the table values, and the average over telescopes is formed.

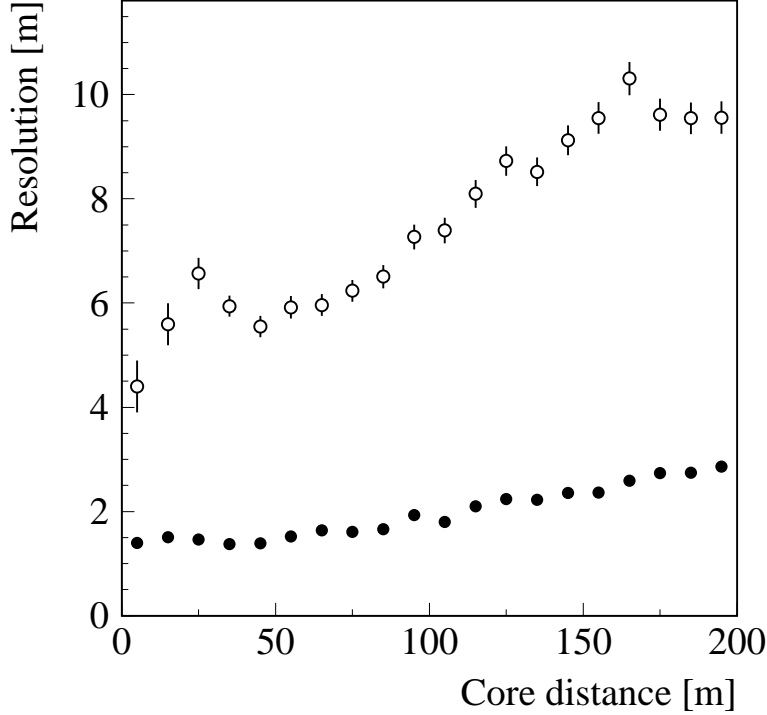


Fig. 6. Resolution in the reconstruction of the core location, projected onto one of the coordinate axes, as a function of the distance of the shower core from the central telescope of the HEGRA IACT system. The simulations assume an energy spectrum similar to the spectrum observed for Mkn 501. Open circles: reconstruction of both the shower direction and the core location. Full circles: reconstruction of the core location, assuming that the shower direction is known.

To account for the dependence on zenith angles, the tables exist for four different zenith angles, and are interpolated.

With this procedure, an energy resolution slightly below 20% is achieved for energies up to 20 TeV (open circles in Fig. 7). At energies beyond 20 TeV, the resolution deteriorates slightly because of the increasing core distances.

Using the information on the shower height, one can change the strategy completely: for a fixed height of the shower maximum, the relation between energy and light yield at a fixed distance from the core should be linear. Therefore, the energy corresponding to a given image *size* I was determined as

$$E = I f(h_{max}, r) t(d_0) g(I) \quad .$$

The basic (tabulated) function f describes the *size/energy* ratio as a function of (measured) shower height h_{max} and radius r ; Fig. 1 in fact shows the values of $1/f$ (in photoelectrons/TeV) for three different ranges in r . Additional correction functions $t(d_0)$ correct for image truncation due to the camera edge, as a function of the *distance* d_0 from the camera center, and for image truncation due to tail cuts, $g(I)$. (Strictly speaking, the intensity lost due to tail cuts is a function not only of image *size* I , but also of the image shape, but for the current purpose the simple correction seemed sufficient.) The energy resolution obtained with this procedure (full triangles in Fig. 7) is improved significantly, and varies between 12% and 14%.

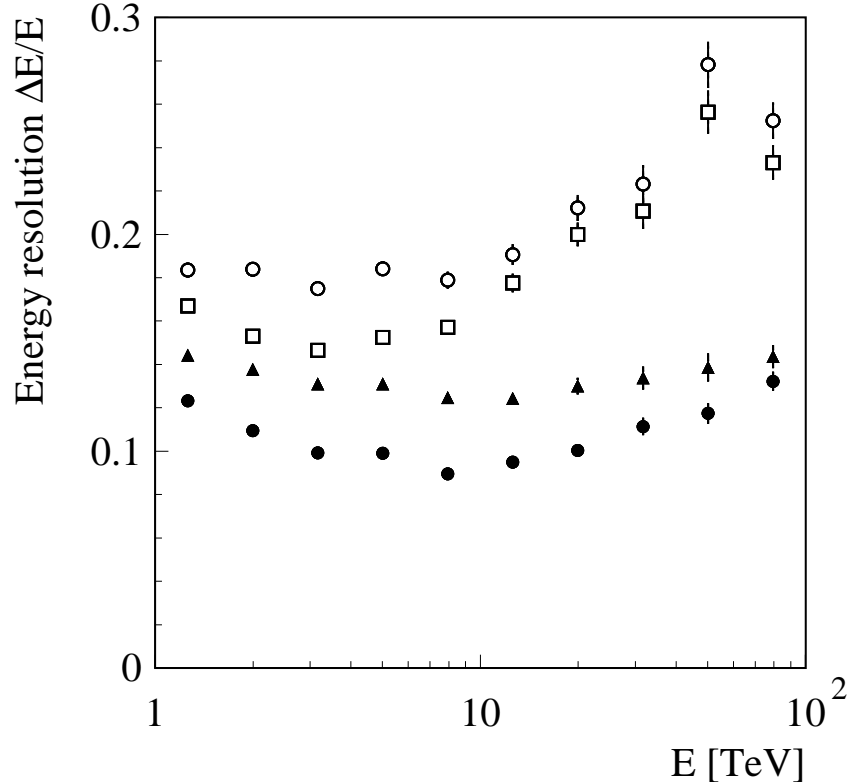


Fig. 7. Energy resolution determined by fitting a Gaussian to the ratio of reconstructed energy to true energy, as a function of the energy of gamma rays. Open circles: conventional energy determination. Full triangles: including the information on the height of the shower maximum. Full circles: using in addition in the core reconstruction the assumption that gamma-rays come from a known point source. Open squares: conventional energy determination, with the core reconstruction assuming a point source.

Using the same procedure, but with the improved determination of the core location on the basis of a known direction of gamma rays, the energy resolution shown as full circles in Fig. 7 is achieved, which now varies between 9% and 12%, almost a factor two better than with the conventional energy reconstruction. We note here that for background events not coming from the source, a wrong energy value will be obtained. However, in a statistical subtraction of background events using a suitable off-source data sample, these events will be canceled no matter how the energy estimate was obtained or how biased it is.

Of course, one can also combine the conventional energy reconstruction with the improved core determination assuming a point source (open squares in Fig. 7); while some improvement is observed, it is clear that the correction for the varying shower height provides the bulk of the improvement, in particular at higher energies.

The technique was also applied to showers at non-zero zenith angles, using events simulated at 20°, 30° and 45° zenith angle. The lookup tables were generated separately for each zenith angle, with an interpolation for intermediate values. The reconstruction techniques - the combination of the shower-height correction and the improved core location - work at all zenith angles. At 10 TeV, e.g., which is well above threshold at all angles, the energy resolution is about 9%

independent of the zenith angle.

7 Concluding remarks

We will first give some caveats, and then add some ideas for further improvement of the energy resolution of IACT systems.

A key issue in the applicability of the energy determination assuming a point source of gamma rays is the mode of failure in case the source is extended, or has an extended component. One will, of course, study the reconstructed angular distributions of gamma-rays; an extended source should be recognized as such if its size is comparable to the angular resolution of the telescopes, of about 0.1° . If a somewhat extended source is mistaken as a point source, the determination of the core location will suffer, and in the extreme case - a source size equivalent to the angular resolution - the gain in the core determination will be lost completely, resulting in a core resolution equivalent to that provided by the normal reconstruction. As a result, the technique provides a soft failure mode in the sense that for marginally extended sources the core resolution and hence the energy resolution will degrade - in the worst case back to the values without the source constraint - but the spectra will not be systematically biased.

Before applying the source constraint, one also needs to make sure that without this constraint the source is reconstructed exactly (within $O(0.01^\circ)$) at the nominal location. Shifts - e.g. due to alignment problems - could generate distortions of the spectrum. In general, the requirements on the alignment of telescopes, both absolute and relative to each other, are increased compared to the normal reconstruction.

Since the entire energy reconstruction is based on correction functions derived from Monte Carlo simulations, one has to ensure that these simulations are correct at the appropriate level of precision. To achieve 10% energy resolution in the actual data sample, it is not sufficient to apply an algorithm which with Monte Carlo events provides this resolution, but one must make sure that radial distributions etc. are indeed correctly predicted, with systematic deviations well below the 10% target resolution. We believe that with the redundant information provided by systems of three or more IACTs, and with the large gamma-ray samples gained e.g. from Mkn 501, one will be able to verify the simulations at such a level. Tests include the comparison of gamma-ray parameters reconstructed using two subsystems of two telescopes each [13], and the comparison of the energies reconstructed by two telescopes at different core distances, in analogy to the technique used in [18] to measure the radial distribution of Cherenkov light.

While the achieved 10% energy resolution is certainly quite acceptable, there are a number of ways further improvements might be reached. For example, the corrections for image truncation are certainly not optimal; using corrections which are optimized for the 1 TeV range, rather than for the entire sample of Monte Carlo events from a few 100 GeV to 100 TeV, the resolution at 1 TeV can be improved by about 1-2%. This suggests an iterative approach, where a first energy estimate is used to select correction functions optimized for the corresponding energy range.

Currently, the available Monte-Carlo statistics limits the detail and dimension of the correction tables. Alternatively, a fit to image templates [15,16] could be used to correct truncation. One could also try to avoid tail cuts entirely in the determination of the image *size*, and generously add border pixels to the images.

The current technique, which uses the information summarized in the Hillas image parameters, exploits for the energy estimate only the information on the height of the shower maximum. Using the full pixel information, one might try to extract the full depth profile of the shower, and include also the higher-order corrections.

In summary, the clear improvement in the energy resolution of IACT systems demonstrates the wealth of information contained in the multiple and redundant images of gamma-ray showers; the techniques presented here should be seen as a first step towards an improved analysis, and almost certainly do not represent the last word.

Acknowledgments

The support of the HEGRA experiment by the German Ministry for Research and Technology BMBF and by the Spanish Research Council CYCIT is acknowledged. We are grateful to the Instituto de Astrofísica de Canarias for the use of the site and for providing excellent working conditions. We thank the other members of the HEGRA CT group, who participated in the construction, installation, and operation of the telescopes, as well as in the analysis and interpretation of data.

References

- [1] T.C. Weekes, Space Science Rev. 75 (1996) 1; M. F. Cawley and T.C.Weekes, Experimental Astronomy 6 (1996) 7.
- [2] G. Mohanty et al., Astropart. Phys. 9 (1998) 15.
- [3] F.W. Samuelson et al., Astrophys. J. 501 (1998) L17.
- [4] F. Aharonian et al., Astron. Astrophys., in print, and astro-ph/9901284 (1999).
- [5] A. Barrau, Ph.D. Thesis, Universite de Grenoble (1998), and A. Barrau et al., astro-ph/9710259.
- [6] F. Aharonian et al., Astron. Astrophys. 342 (1999) 69.
- [7] A. Barrau et al., astro-ph/9710259 (1997), and A. Barrau, Ph.D. Thesis, Grenoble (1998).
- [8] N. Hayashida et al., Astroph. J. 504 (1998) L71.
- [9] G. Hermann, Proceedings of the Int. Workshop “Towards a Major Atmospheric Cherenkov Detector IV”, Padua, (1995), M. Cresti (Ed.), p. 396.

- [10] A. Daum et al., *Astropart. Phys.* 8 (1997) 1.
- [11] N. Bulian et al., *Astropart. Phys.* 8 (1998) 223.
- [12] A. Konopelko, *Astropart. Phys.*, in print, and astro-ph/9901365.
- [13] W. Hofmann, Proceedings of the Int. Workshop “Towards a Major Atmospheric Cherenkov Detector V”, Kruger Park, (1997), p. 284, and astro-ph/9710297 (1997).
- [14] W. Hofmann et al., submitted to *Astroparticle Physics*, and astro-ph/9904234.
- [15] M. Ulrich et al., *J. Phys. G* 24 (1998) 883.
- [16] S. Le Bohec et al., *Nucl. Instr. Meth.* A416 (1998) 425.
- [17] F. Krennrich, R.C. Lamb, Proceedings of the Int. Workshop “Towards a Major Atmospheric Cherenkov Detector IV”, Padua, (1995), M. Cresti (Ed.), p. 405.
- [18] F. Aharonian et al., *Astropart. Phys.* 10 (1999) 21.